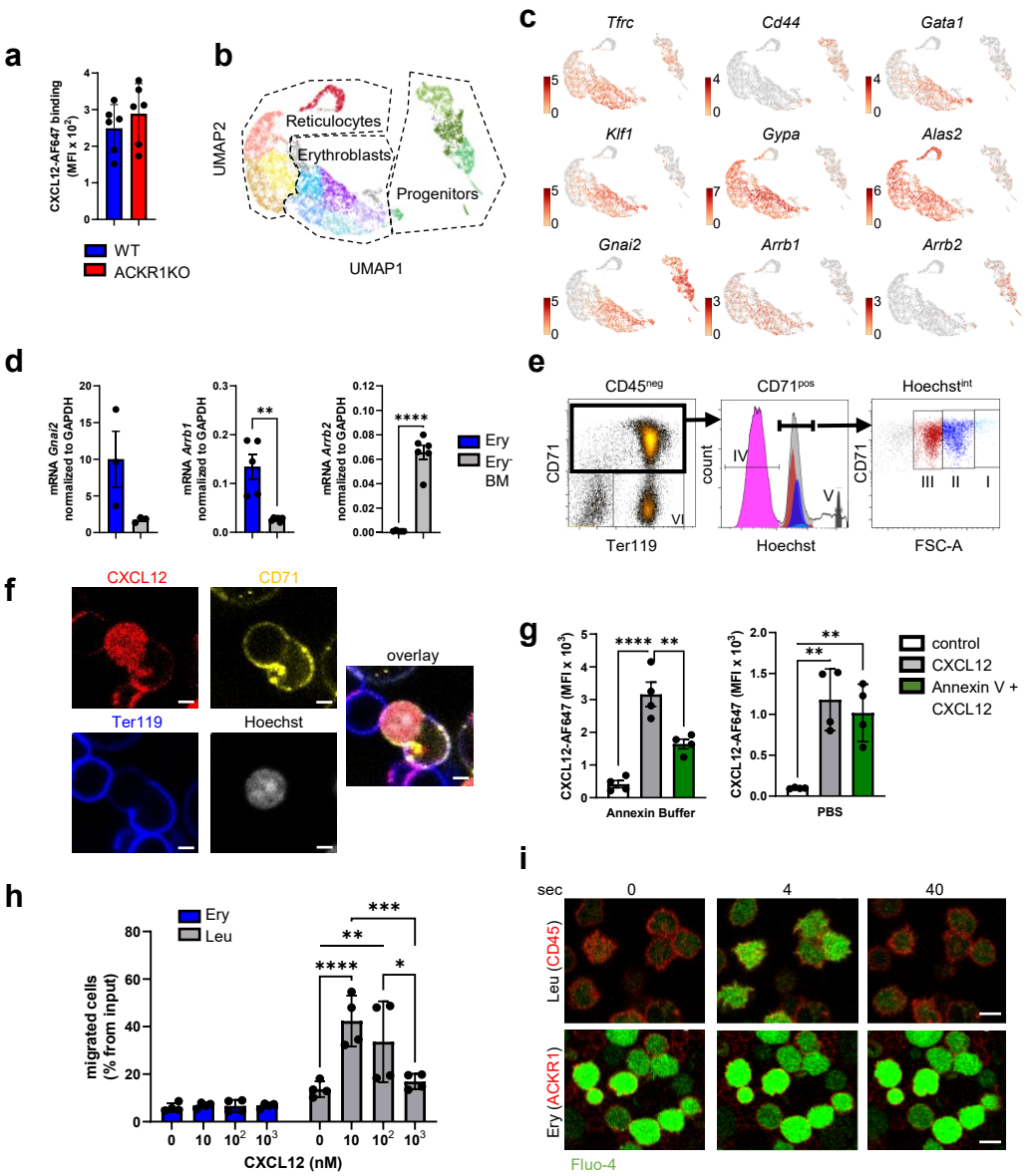

Extended Data Figure 1. Molecular makeup and CXCR4-induced responses of bone marrow erythroid cells.

a, CXCL12-AF647 binding to bone marrow CD71⁺Ter119⁺ erythroblasts from WT and ACKR1-knockout (KO) mice measured in flow cytometry (n = 6 mice; * p<0.05 paired two-tailed t-test). **b,** UMAP projections of scRNAseq of CD71⁺ bone marrow cells from a WT mouse identified multiple clusters, grouped as follows: progenitors (*Tfrc⁺, Cd44⁺)* erythroblasts (*Tfrc^{high}, Gata1^{high}, Klf1^{high})* and reticulocytes *(Gypa^{high}, Alas2^{high})*. **c,** Log2 transcription of *Tfrc, Cd44, Gata1, Klf1 Gypa, Alas2, Gnai2, Arrb1* and *Arrb2* from scRNAseq of CD71⁺ bone marrow cells. **d,** Abundance of *Gnai2, Arrb1* and *Arrb2* transcripts in Ter119⁺ erythroid cells (Ery) and Ery-depleted bone marrow cells (Ery⁻ BM) measured by qPCR (normalized to GAPDH; *Gnai2 n* = 3, *Arrb1* and *Arrb2 n* = 5 mice; ** p<0.01, **** p<0.001 unpaired two-tailed t-test). **e,** Flow cytometry gating strategy to define CD45⁻ erythroid subpopulations in murine bone marrow: proerythroblasts (I), early erythroblasts (II), late erythroblasts (III), reticulocytes (IV), pyrenocytes (V) and erythrocytes (VI). **f,** CXCL12-AF647 binding to a pyrenocyte in confocal microscopy (CXCL12, red; CD71, yellow; Ter119, blue; nucleus, Hoechst, white) Scale bars, 2 µm. **g,** CXCL12-AF647 binding to bone marrow pyrenocytes with and without Annexin V measured in flow cytometry, **left**: in Annexin buffer, **right** in PBS (n = 4 mice; ** p<0.01, **** p<0.001 in one-way ANOVA with Tukey's multiple comparisons test). **h,** CXCL12-induced migration of CD71⁺Ter119⁺ erythroblasts (Ery) and leukocytes (Leu) after 3 hours in a Transwell assay (n = 4 mice; * p<0.05, ** p<0.01, **** p<0.001 in two-way ANOVA with Tukey's multiple comparisons test). **i,** Live cell imaging, of free intracellular calcium detected after CXCL12 stimulation by Fluo-4 fluorescence (green); **top,** Leukocytes, CD45⁺ (red); **bottom**, Erythroid cells, ACKR1 (red) at 0, 4 and 40 seconds, left, middle and right panels, respectively. Scale bars, 10 µm. Also, in **Video 1** and **Video 2.** Data are shown as mean ± sem., each data point represents one mouse.

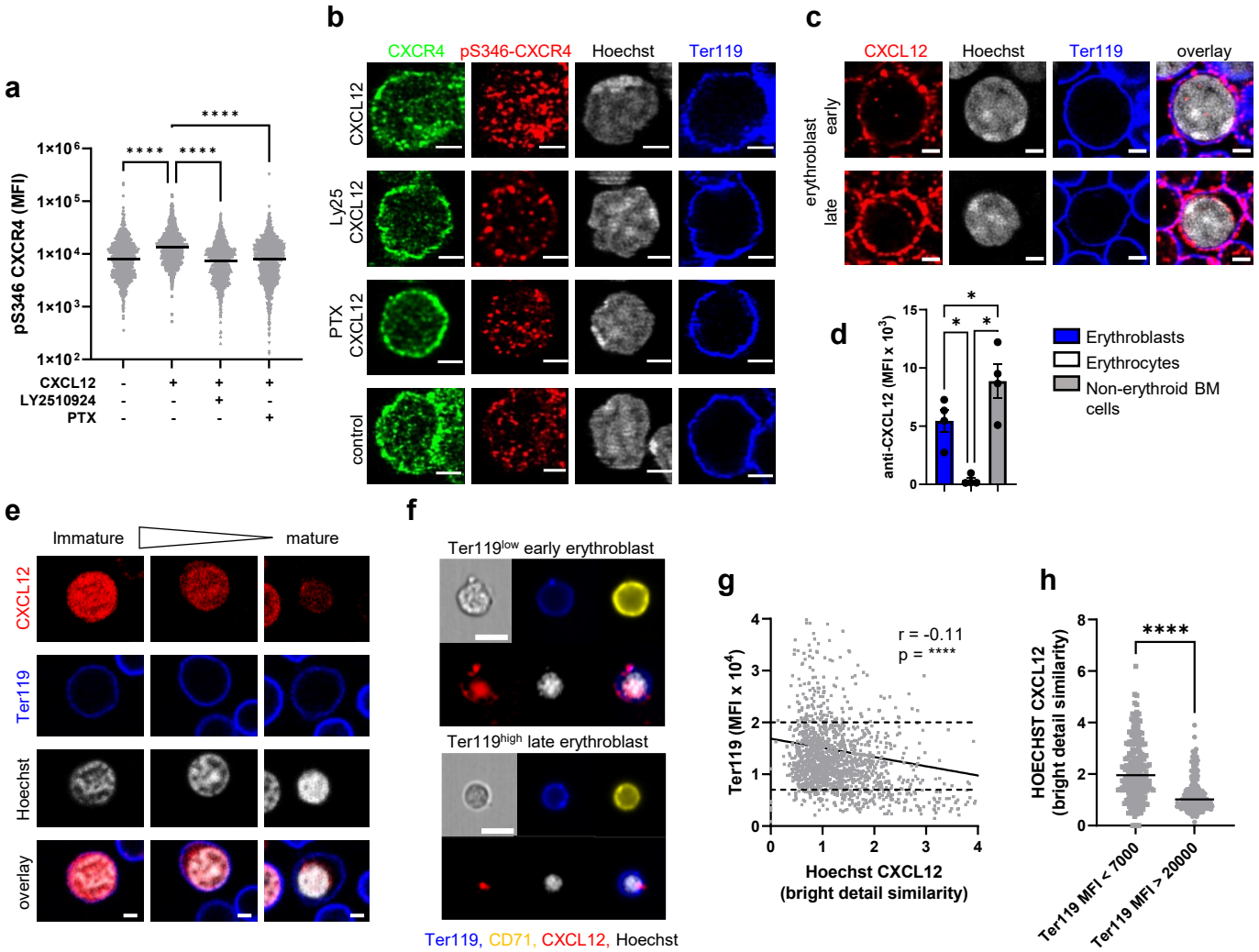

Extended Data Figure 2. CXCL12-induced CXCR4 phosphorylation and its nuclear localization in erythroblasts.

a, Mean fluorescence intensity (MFI) of anti-pS346-CXCR4 antibody staining of freshly isolated CD71⁺Ter119⁺ bone marrow erythroblasts stimulated with CXCL12 with and without either CXCR4-antagonist LY2510824, or pertussis toxin (PTX), and analyzed in imaging flow cytometry. Individual and median values for 655-1193 cells per group are shown for one experiment out of three replicates (**** $p<0.001$ in one-way ANOVA with Tukey's multiple comparisons test). **b,** Confocal images of 0.2 µm optical sections of freshly-isolated murine bone marrow erythroblasts stimulated with CXCL12 and stained with anti-CXCR4 antibody (green), anti-pS346 CXCR4 antibody (red), anti-Ter119 antibody (blue) and Hoechst (white) with or without pre-treatment with either LY2510824 or PTX. Scale bars, 5 µm. **c,** Anti-CXCL12 antibody reactivity (red) in untreated freshly isolated Ter119-positive (blue) early (**top**) and late (**bottom**) bone marrow erythroblasts as categorized by the size and density of their nuclei. Scale bars, 5 µm. **d,** Endogenous cell-associated CXCL12 quantified in bone marrow cell populations by flow cytometry using anti-CXCL12 antibody (Mean ± sem shown, n = 4 mice; * $p<0.05$ in one-way ANOVA with Tukey's multiple comparisons test). **e,** Confocal images illustrating CXCL12-AF647 (red) internalization by proerythroblast (**left**), early erythroblast (**middle**), late erythroblast (**right**), defined by the size and density of their nuclei. Ter119 (blue) and Hoechst (white). Scale bars, 2 µm. **f,** CXCL12-AF647 (red) internalization by early- and late-stage erythroblasts in imaging flow cytometry. Ter119 (blue), CD71 (yellow) and Hoechst (white). Scale bars, 10 µm. **g,** Linear regression between Ter119 MFI and Hoechst-CXCL12 bright detail similarity measured by imaging flow cytometry. Dotted lines delineate top and bottom 14 % of Ter119 expressing 1563 cells from 1 experiment of 3 replicates. Solid line shows simple linear regression. **h,** Median bright detail similarity of CXCL12-AF647 and Hoechst in early and late erythroblasts, 212 and 218 cells, respectively. **** $p<0.001$ in unpaired two-tailed t-test.

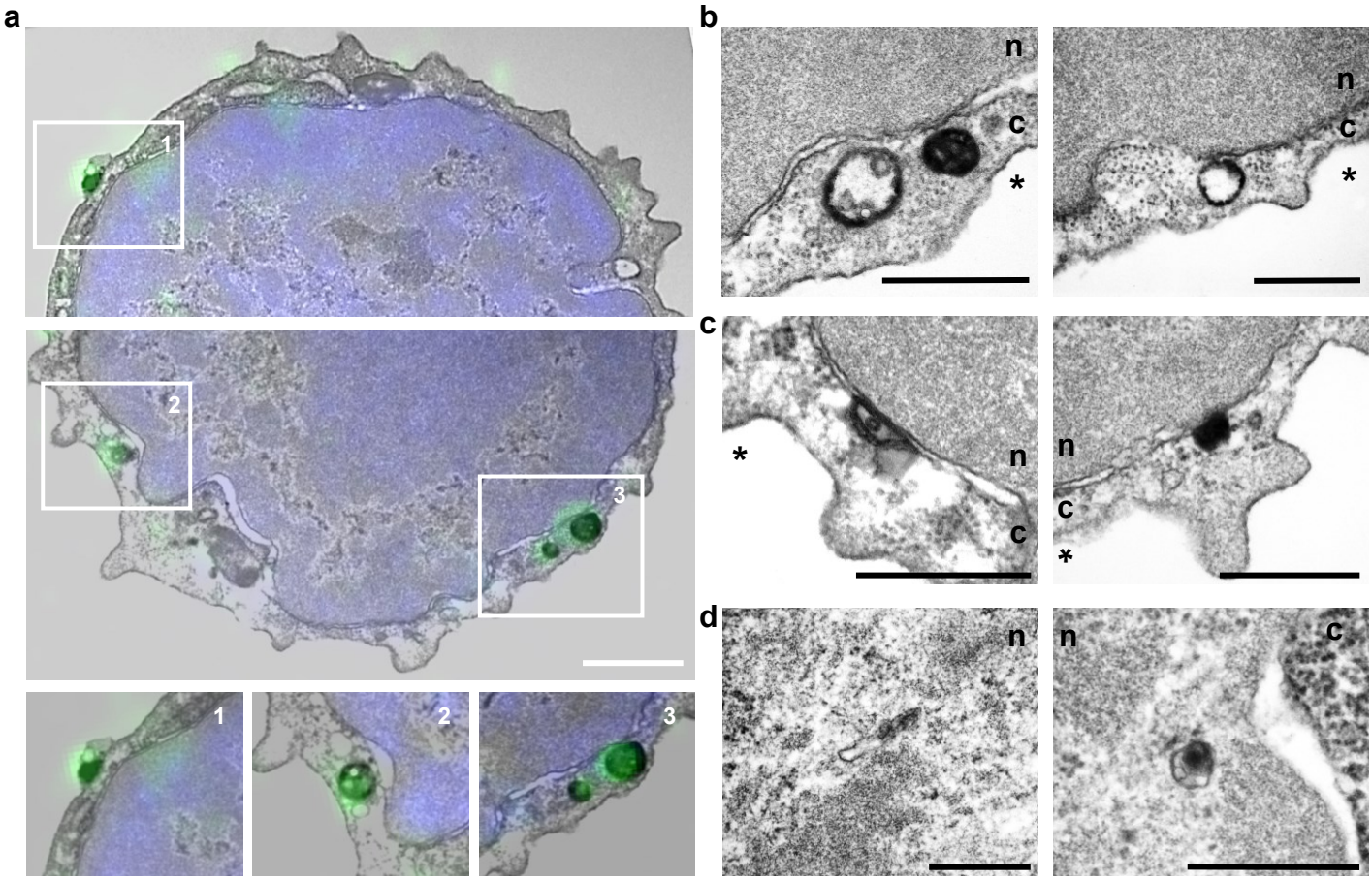

Extended Data Figure 3. Subcellular localization of CXCR4 in erythroblasts in correlative fluorescence and immune-electron microscopy.

a, Subcellular localization of two CXCR4-associated immune-labels in an erythroblast observed by correlative confocal immunofluorescence microscopy and by transmission immune-electron microscopy, representative of 8 cells observed. Image shows two segments of an erythroblast at different z-depth. Freshly isolated viable erythroblasts were stimulated with CXCL12, pulsed with rat anti-CXCR4-AF488 and a horseradish peroxidase (HRP)-labeled goat-anti-rat Ig antibody and counterstained with Hoechst. The fluorescent signal was detected in 0.3 µm optical confocal microscopy sections, anti-CXCR4-AF488 (green) and Hoechst (blue). The HRP was visualized by its substrate 3,3-diaminobenzidine (DAB) that was biocatalyzed to form an electron-dense precipitate detected in ultrathin sections by transmission electron microscopy. The confocal and ultrastructural images were digitally aligned. Scale bar, 1 µm. Separated fluorescent and electron microscopy images are in **Supplementary Fig. 1 c,d**. **Area 1** shows CXCR4 endocytosis from the membrane**. Areas 2** and **3** show $CXCR4^{+}$ large multivesicular bodies in close proximity and associated with the nuclear membrane. **b-d,** CXCR4-associated signal in erythroblasts detected in transmission electron microscopy as an electron-dense DAB precipitate in **b,** multivesicular bodies associated with the nuclear envelope; **c,** on the outer layer of the nuclear envelope; **d,** in the nucleoplasmic reticulum. In **b-d,** nucleus (n), cytoplasm (c), extracellular space (*). Scale bars, 0.5 µm.

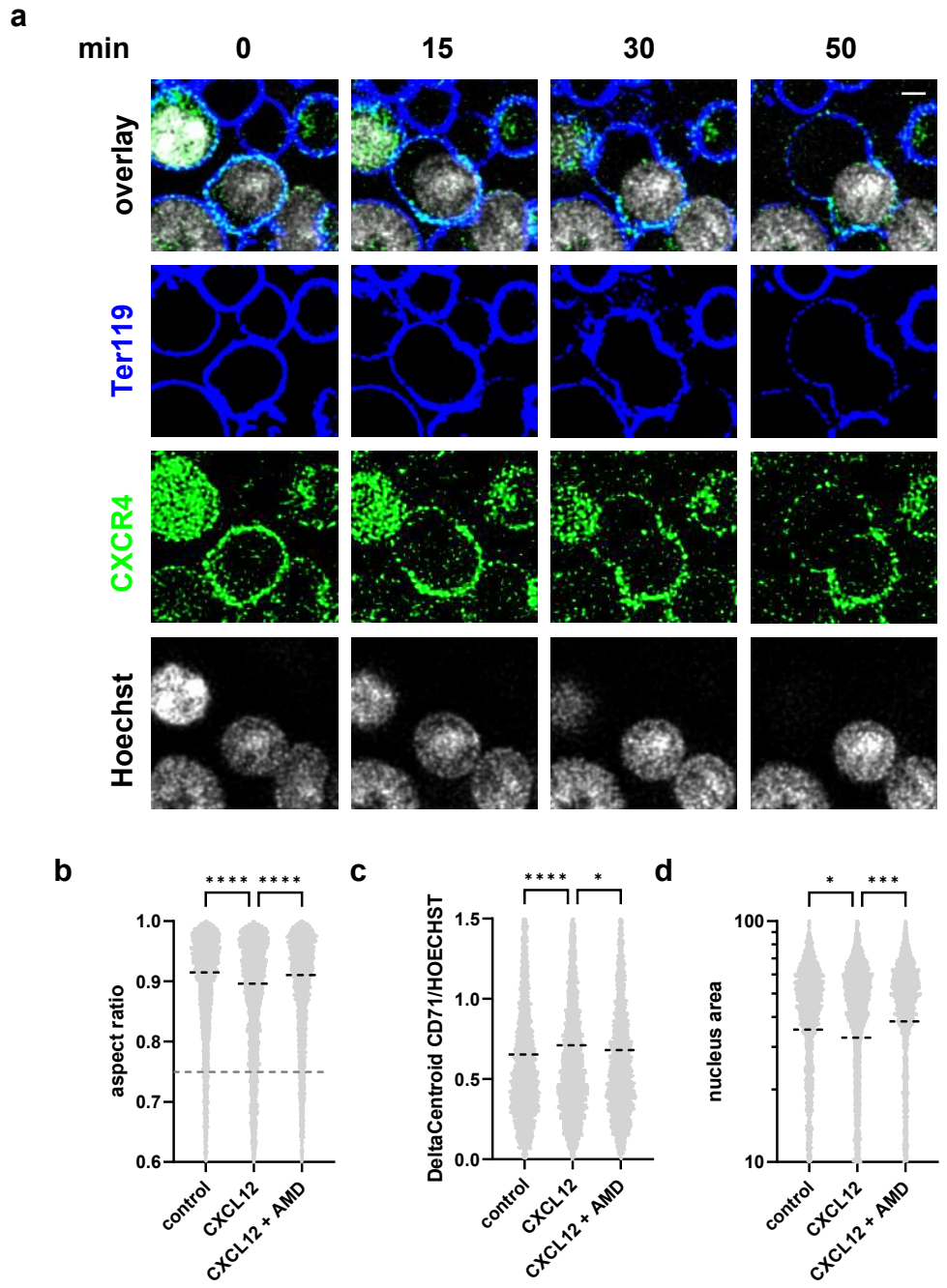

Extended Data Figure 4. CXCL12 triggers erythroblast elongation, CXCR4 redistribution, nuclear polarization and chromatin condensation.

a, Live cell imaging of bone marrow-derived erythroblasts pre-labeled with anti-CXCR4 antibody (green), anti-Ter119 antibody (blue) and nuclear dye Hoechst (white) with CXCL12 added during imaging. Also, in **Video 5**. Scale bar, 2 µm. **b-d,** Imaging flow cytometry analysis of bone-marrow derived erythroblasts treated with CXCL12, alone or with AMD3100, showing calculated **(b)** cell aspect ratios (dotted line delineates elongated erythroblast with aspect ratios of 0.75 or lower); **(c)** dislocation of the nucleus from the cell center, measured as a delta-centroid of CD71 and Hoechst stains and **(d)** nucleus area, measured as the size of Hoechst stain. Cumulative results from three individual experiments on cells of one mouse (total 3357 and 4210 cells per group). * $p<0.05$, *** $p<0.005$, **** $p<0.001$ in one-way ANOVA with Tukey's multiple comparison tests.

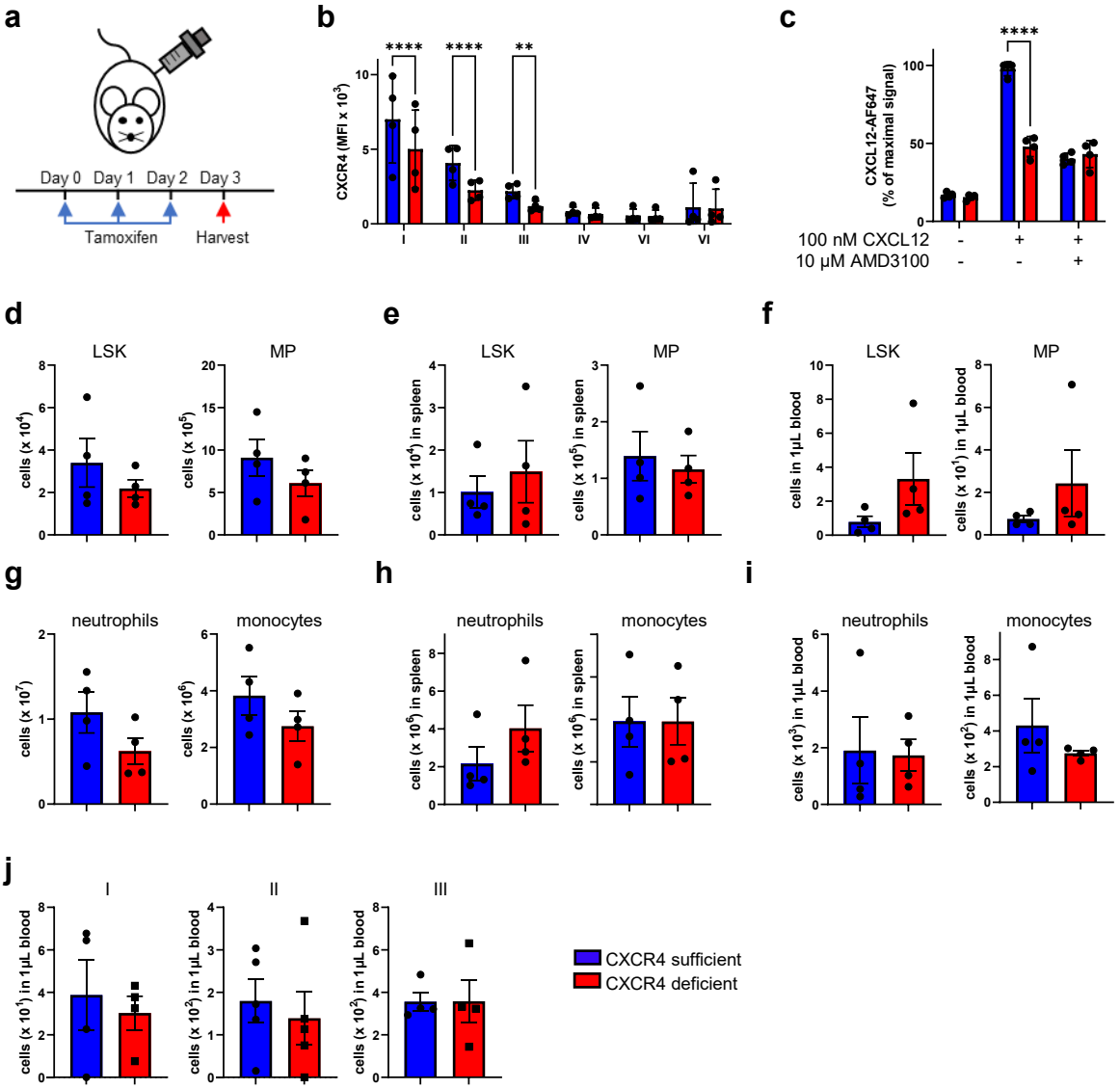

Extended Data Figure 5. CXCR4 depletion and cell counts in CXCR4-floxed UBC-ERT2-Cre mouse model. **a,** Schematic representation of *in vivo* tamoxifen treatment protocol of CXCR4 floxed UBC-ERT2 Cre (CXCR4-deficient) and CXCR4 floxed (CXCR4-sufficient) mice. **b,** Anti-CXCR4 antibody reactivity with murine bone marrow proerythroblasts (I), early erythroblasts (II), late erythroblasts (III), reticulocytes (IV), pyrenocytes (V) and erythrocytes (VI) from CXCR4 sufficient and deficient mice measured by flow cytometry (n = 4 mice per group; ** p<0.01, **** p<0.001 in two-way ANOVA with Šídák's multiple comparisons test). **c,** CXCL12-AF647 binding and its inhibition by CXCR4 antagonist AMD3100 in early erythroblasts from CXCR4 sufficient and deficient mice measured by flow cytometry (n = 4 per group; **** p<0.001 in two-way ANOVA with Šídák's multiple comparisons test). Total number of Lineage$^-$ Sca1$^+$c-kit$^+$ cells (LSKs) and myeloid progenitors (MPs) in **d,** bone marrow (6 bones); **e,** whole spleen; and **f,** 1 µL blood of CXCR4-sufficient and -deficient mice. Total number of neutrophils and monocytes in **g,** bone marrow (6 bones); **h,** whole spleens; **i,** 1 µL blood of CXCR4 sufficient and deficient mice. **j,** Total number of proerythroblasts (I), early erythroblasts (II), late erythroblasts (III) in 1 µL blood from CXCR4 sufficient and deficient mice. **d-j**, Unpaired two-tailed t-tests (n = 4 mice per genotype).